

# SCIENTIFIC REPORTS



OPEN

## Interaction driven quantum Hall effect in artificially stacked graphene bilayers

Muhammad Zahir Iqbal<sup>1,2,3</sup>, Muhammad Waqas Iqbal<sup>2,4</sup>, Salma Siddique<sup>5</sup>,  
Muhammad Farooq Khan<sup>2</sup>, Shahid Mahmood Ramay<sup>6</sup>, Jungtae Nam<sup>2</sup>, Keun Soo Kim<sup>2</sup> &  
Jonghwa Eom<sup>2</sup>

Received: 30 April 2015

Accepted: 01 April 2016

Published: 21 April 2016

The honeycomb lattice structure of graphene gives rise to its exceptional electronic properties of linear dispersion relation and its chiral nature of charge carriers. The exceptional electronic properties of graphene stem from linear dispersion relation and chiral nature of charge carriers, originating from its honeycomb lattice structure. Here, we address the quantum Hall effect in artificially stacked graphene bilayers and single layer graphene grown by chemical vapor deposition. The quantum Hall plateaus started to appear more than 3T and became clearer at higher magnetic fields up to 9T. Shubnikov-de Hass oscillations were manifestly observed in graphene bilayers texture. These unusual plateaus may have been due to the layers interaction in artificially stacked graphene bilayers. Our study initiates the understanding of interactions between artificially stacked graphene layers.

The robust electronic properties of graphene stem from linear dispersion relation, containing massless Dirac fermions and chiral nature of charge carriers. This behavior of graphene originates from its honeycomb lattice structure. Bernal stacked bilayers graphene consists of massive Dirac fermions spectrum, which is demonstrated by two pairs of parabolic bands<sup>1–3</sup>. The massless Dirac spectrum could be expectedly present in bilayers graphene if both layers were precisely placed with AA-stacking symmetry<sup>4,5</sup>. The stacking of more graphene layers are useful for vertical transport which enhance the spin signal<sup>6,7</sup>. The structural distortion in the layers is manifested to the formation of correlated states and therefore the distortion can be created by applying strain<sup>8,9</sup>, as stacking one layer on top of another layer<sup>10–15</sup>. This artificial stacking of graphene bilayers is usually expected to be unstable towards symmetry breaking due to the twist angle. The recent reports showed that a very small distribution is sufficient enough to generate a completely new electronic spectrum with broken symmetry<sup>16</sup>. The interlayer Coulomb interactions and tunneling effects of the two closely spaced graphene layers may lead to a new interesting phenomena. The new phenomenon is similar to the bilayers of two dimensional electron gas; which not present in individual layers<sup>17–19</sup>. Perhaps due to the Fermi surface of carbon it is possible where the honeycomb lattice in graphene are centered at nonzero K vectors<sup>20</sup> and relative disparity between the layers resulting in weak coupling<sup>21</sup>. The effect of symmetry breaking of graphene and its significant in electronic transport properties is an enduring topic to identify the various ground states.

The electrical transport such as quantum Hall effect in single and Bernal stacked bilayers graphene has been explored to a large extent. However, it is interesting to investigate the electronic transport properties of artificially stacked graphene layers. Here we report the electronic transport properties of artificially stacked chemical vapor deposition grown graphene bilayers. We have observed that the quantum Hall effect consisting of various plateaus with non-integer quantized values at 4.2 K, however a typical massless Dirac fermions spectrum has observed in a single layer graphene. The clear quantum Hall plateaus started to appear from 3 T in graphene bilayers and became more prominent at higher magnetic fields. The Shubnikov-de Hass (SdH) oscillations were observed as well in graphene bilayers texture.

<sup>1</sup>Faculty of Engineering Sciences, GIK Institute of Engineering Sciences and Technology, Topi 23640, Khyber Pakhtunkhwa, Pakistan. <sup>2</sup>Department of Physics & Graphene Research Institute, Sejong University, Seoul 143-747, Korea. <sup>3</sup>Department of Physics & Astronomy, Georgia State University, Atlanta, GA 30303, USA. <sup>4</sup>Department of Physics, College of Science, Majmaah University, Al-Zulfi 11932, Saudi Arabia. <sup>5</sup>Department of Bioscience & Biotechnology, Sejong University, Seoul 143-747, Korea. <sup>6</sup>Physics & Astronomy Department, College of Science, King Saud University, Riyadh 11451, Saudi Arabia. Correspondence and requests for materials should be addressed to M.Z.I. (email: zahir.upc@gmail.com)

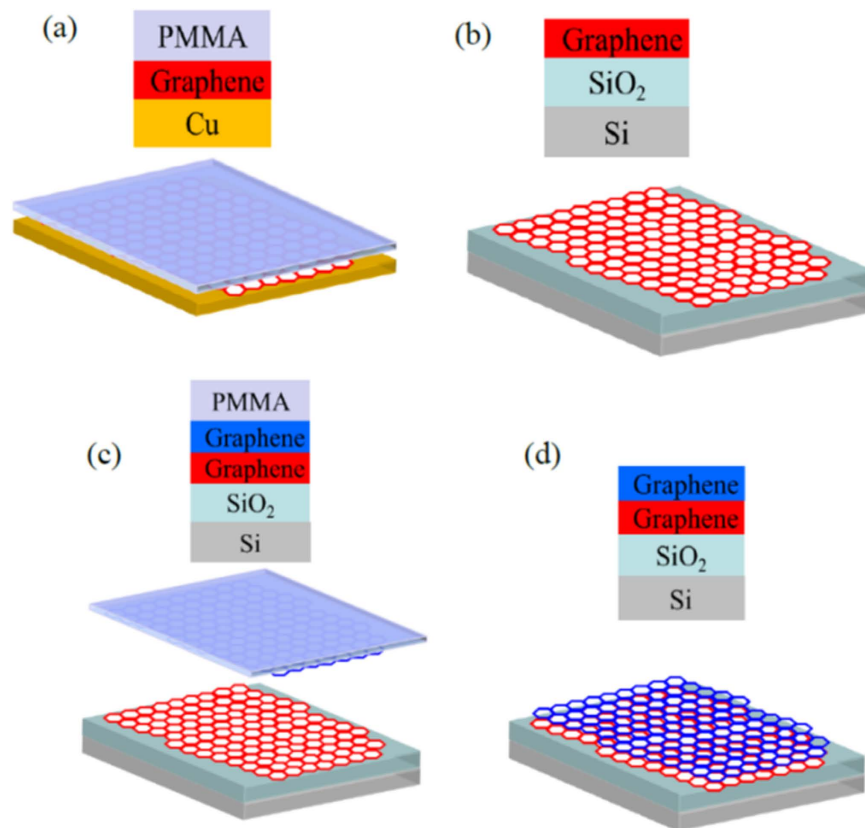


**Figure 1. Schematic of artificially stacked graphene bilayers with top layer having twist angle.** (a) Graphene on Cu foil with PMMA coating. (b) Graphene transferred on the SiO<sub>2</sub>/Si substrate. (c) Second graphene layer coated with PMMA subsequently transferred to the first layer. (d) Graphene bilayers transferred to the SiO<sub>2</sub>/Si substrate.

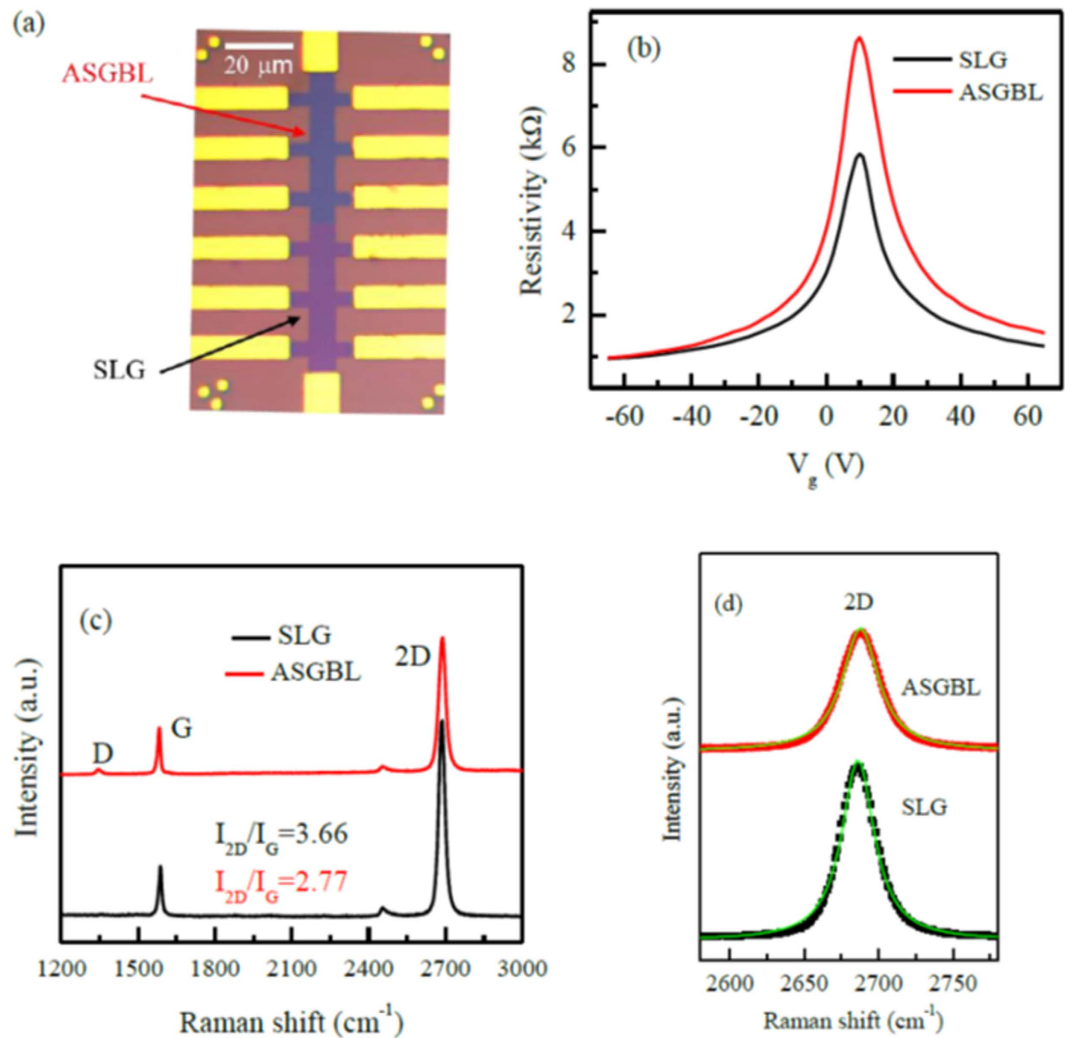
## Results and Discussion

Figure 1 shows a schematic steps and the optical image of two mis-oriented graphene layers on SiO<sub>2</sub>/Si substrate. Figure 1(a) shows the CVD grown graphene on Cu foil with PMMA coating. The second step is the transferred of graphene to SiO<sub>2</sub>/Si substrate as displayed in Fig. 1(b). The second graphene layer coated with PMMA is subsequently transferred to the first graphene layer to make it bilayers shown in Fig. 1(c). The complete schematic of graphene bilayers after removing PMMA is presented in Fig. 1(d). The bottom layer of graphene has shown in red color honey combs while the top graphene layer has represented by the color blue.

The optical micrograph image of complete Hall bar device structure with Au electrodes has shown in Fig. 2(a). Where the dark part of Hall bar device represents the bilayers graphene region and slightly the light color indicate the single layer graphene. The resistivity as the function of back gate voltage for artificially stacked graphene bilayers (ASGBL) device and a single layer graphene (SLG) region has shown in Fig. 2(b). The field effect hole and electron mobility values of the single layer region of graphene device have found to be around 2363 and 2060 cm<sup>2</sup>/Vs, respectively; while the field effect hole and electron mobility values of the double-layer region of graphene device at 0 T appeared to be about 2058 and 1625 cm<sup>2</sup>/Vs at temperature of 4.2 K, respectively. Figure 2(c) shows the Raman spectra of SLG and ASGBL. The 2D/G peak intensity ratio ( $I_{2D}/I_G$ ) value is  $\sim 3.66$  for the case of SLG and  $\sim 2.77$  for ASGBL as shown in the Fig. 2(c). The D-like peak is observed due to the twist angle between two graphene layers and similar kind of peaks have been observed previously in the twisted bilayers graphene as reported by C. C. Lu *et al.*<sup>22</sup>. The full width half maxima (FWHM) of 2D peaks for both SLG and ASGBL estimated by Lorentz fitting are about  $\sim 26$  and  $\sim 29$  cm<sup>-1</sup>, respectively as shown in Fig. 2(d).

Figure 3(a) shows the longitudinal resistivity ( $\rho_{xx}$ ) and Hall conductivity ( $\sigma_{xy}$ ) of SLG as a function of applied back-gate voltage ( $V_g$ ), with magnetic field (B) of 9 T at 4.2 K. The result showed a strong evidence of quantum Hall effect (QHE) with conductivity plateaus appeared at  $\pm 2$ ,  $\pm 6$ ,  $\pm 10$ ,  $\pm 14$ ,  $\pm 18$ , together with resistivity minima, consistent with the Landau level spectrum expected for SLG graphene<sup>23</sup>. In the case of ASGBL has also showed the QHE plateaus with different conductivity values as shown in Fig. 3(b). These plateaus revealed an unusual trend, which is different from the single layer or the Bernal stacked bilayers graphene<sup>2,23</sup>. Therefore, these observations refer to a perturbed system that may be due to interaction between two graphene layers.

Figure 4(a) shows the longitudinal resistivity as a function of applied back-gate voltage from 0 to 9 T at 4.2 K. At the lower magnetic field up to 3 T no evident peak is observed, the resistivity plots are similar as 0 T. However, under application of high magnetic fields, transport measurements show a spectrum of symmetric oscillations on the each side of Dirac point with resistivity minima by increasing the applied back-gate voltage. At fields larger



**Figure 2.** (a) Optical microscope image of graphene Hall bar patterns of artificially stacked graphene bilayers (ASGBL) and single layer graphene (SLG) region. (b) Resistivity as a function of back gate voltage ( $V_g$ ) for ASGBL and SLG. (c) Raman spectra of ASGBL and SLG region shows the 2D-to-G ratio of 3.66 and 2.77  $\text{cm}^{-1}$ , respectively. (d) Lorentz fitting to the 2D peaks of ASGBL and SLG to estimate the full width half maxima.

than 3 T, the plateaus are started to appear and became clearer at higher magnetic fields up to 9 T, indicative of the high quality of our sample. Figure 4(b) shows the Hall conductivity as a function of the charge carrier density induced by the applied back-gate voltage in the magnetic field range from 0 to 9 T (with step of 1 T), at 4.2 K. The total density is calculated from  $n = C_g(V_g - V_{\text{Dirac}})/e$ , where  $C_g/e = 7.19 \times 10^{10} \text{ cm}^{-2}\text{V}^{-1}$  and  $V_{\text{Dirac}} = +10 \text{ V}$  is the offset voltage to reach charge neutrality<sup>24</sup>. The transverse transport measurements show the development of quantum Hall states (QHSs) which are consistent with vanishing resistivities as shown in Fig. 4(a).

Figure 5 (a) shows a comparison of quantum Hall measurements of the longitudinal ( $\rho_{xx}$ ) and the Hall resistivity ( $\rho_{xy}$ ) as a function of magnetic field at local back gate voltage of  $-40 \text{ V}$ . Interestingly, this complex system of artificially stacked graphene bilayers shows the Shubnikov-de Haas oscillation. The resulting data ( $\rho_{xx}$  vs.  $B$ ) reveal SdH oscillations which starts from magnetic fields as low as  $B \sim 3 \text{ T}$  and it is consistent with Fig. 3 data, where QHSs are visible at the same  $B$  fields. Furthermore, the longitudinal resistivity against  $V_g$  and  $B$  data which follows the quantum Hall states randomly as a monolayer ( $\nu = \pm 2, 6, 10, 14, 18, 22, \dots$ ) or bilayers ( $\nu = \pm 4, 8, 12, 16, 20, 24, \dots$ ). The contour plot of longitudinal resistivity ( $\rho_{xx}$ ) as a function of  $V_g$  and  $B$  is shown in Fig. 5(b). The black lines are representing observed filling factor positions of ASGBL at ( $\nu = \pm 4, 6, 10, 14, \dots$ ). Some previous studies of artificially stacked or twisted bilayers graphene describe the parallel conduction through each monolayers, while the other results follow the four-fold or eight-fold degeneracy<sup>25–27</sup>. As the unusual perturbation due to the layer interaction has been predicted by the angle resolved photoelectron spectroscopy (ARPES). Experiments that refer to the symmetry-broken bilayers graphene as reported by K. S. Kim *et al.*<sup>16</sup> and theoretically predicted by M.-Y. Choi *et al.*<sup>28</sup>. Although, the theoretical observation of Landau-level spectra in twisted bilayers graphene has reported by Z. F. Wang *et al.*<sup>29</sup>. In the light of above mentioned experiments the hierarchy of Dirac fermions are significantly related to charge transport due to the combination of massive and massless fermions and the quantum transport phenomenon such as valley Hall effect in multiband complex system.

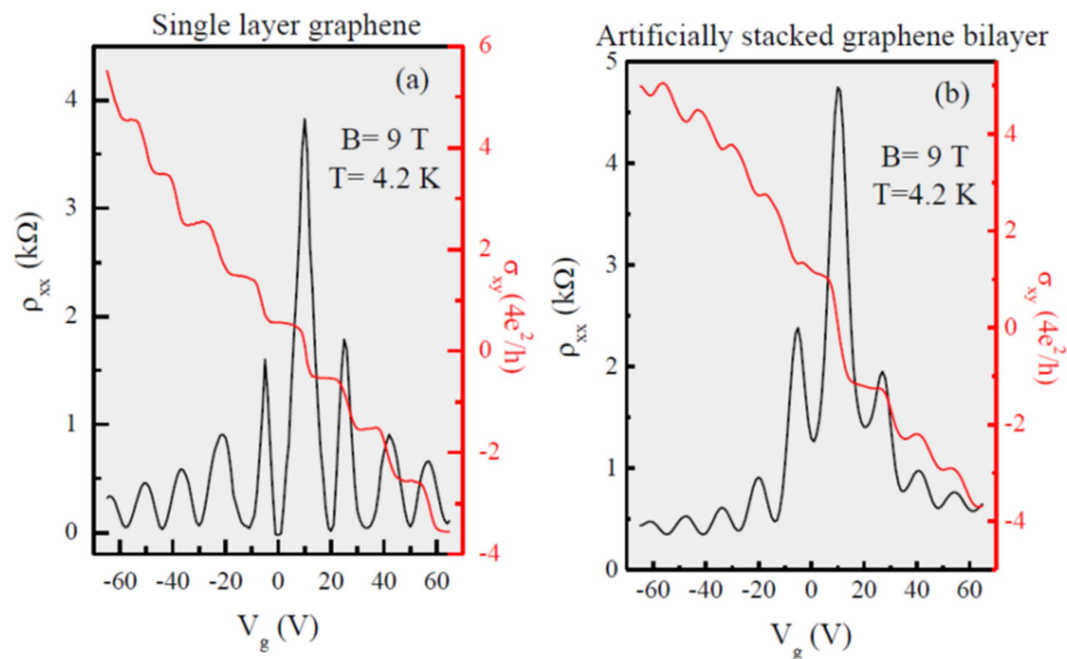


**Figure 3.** The longitudinal resistivity and Hall conductivity of as a function of applied back-gate voltage ( $V_g$ ) with magnetic field of 9 T at 4.2 K (a) Single layer graphene (b) Artificially stacked graphene bilayers.

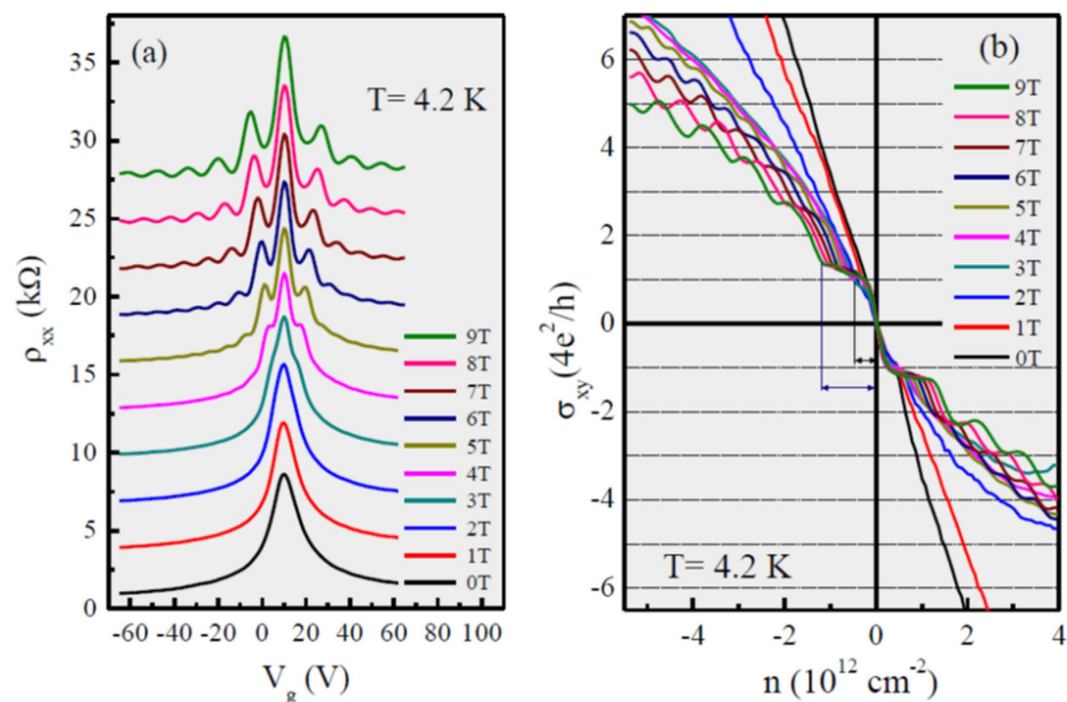


**Figure 4.** (a) The longitudinal resistivity as a function of the back-gate voltage and (b) Hall conductivity as a function of the charge carrier density from 0 to 9 T (with step of 1 T) at 4.2 K.

## Conclusion

In summary, we have studied the structural and electrical transport properties of chemical vapor deposition grown single layer graphene and artificially stacked graphene bilayers. The typical massless Dirac fermions spectrum is observed in the quantum transport of single layer graphene, however artificially stacked graphene bilayers texture follows the quantum Hall states randomly as a monolayer or bilayers at 4.2 K. The hierarchy of Dirac fermions are significantly related to charge transport due to the combination of massive and massless fermions.

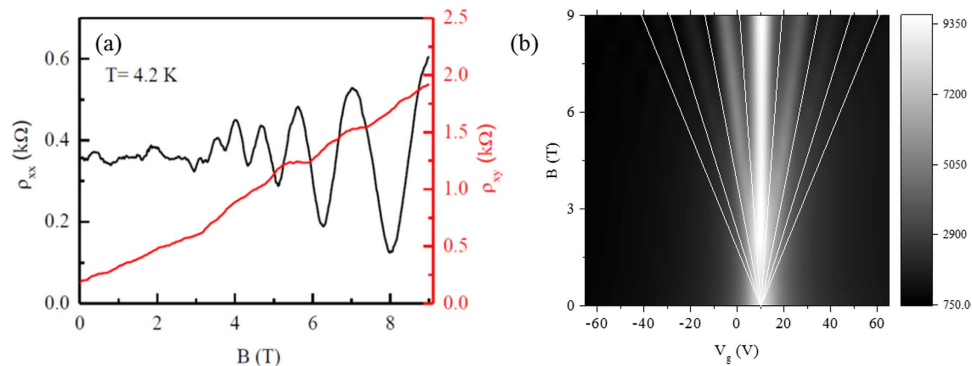


**Figure 5.** (a) The quantum Hall measurements of the longitudinal ( $\rho_{xx}$ ) and the Hall resistivity ( $\rho_{xy}$ ) as a function of magnetic field at local back gate voltage of  $-40$  V. (b) The contour plot of longitudinal resistivity ( $\rho_{xx}$ ) as a function of  $V_g$  and  $B$ .

The unusual Dirac fermion spectrum may have possibly caused by the layers interaction in artificially stacked graphene bilayers.

## Methods

**Graphene growth and device fabrication.** Graphene film was grown on 25- $\mu\text{m}$ -thick copper foils from Alfa Aesar (99.8% pure) via thermal CVD. A mechanically polished and electropolished copper foil was inserted into the CVD furnace. The furnace was evacuated to  $\sim 10^{-4}$  Torr, and the temperature rose to 1010  $^{\circ}\text{C}$  with  $\text{H}_2$  gas flow ( $\sim 10^{-2}$  Torr). After the temperature stabilized at 1010  $^{\circ}\text{C}$ ,  $\text{CH}_4$  and  $\text{H}_2$  (20 and 5 standard cubic centimeters per minute, respectively) were injected into the furnace to synthesize the graphene for 8 min, after which the sample was cooled at a rate of 50  $^{\circ}\text{C}/\text{min}$  to room temperature<sup>30</sup>. The graphene film grown on Cu foil was transferred to a Si substrate by the wet transfer method. The Cu foil was spin-coated (850 rpm for 10 s, 2500 rpm for 30 s) with a thin layer of polymethylmethacrylate (PMMA). Then, the bottom Cu foil was removed by etching in a 1 M solution of ammonium persulfate (APS,  $(\text{NH}_4)_2\text{S}_2\text{O}_8$ ), and the PMMA membrane was washed with deionized water. Next, the graphene film with the PMMA membrane was transferred to the p-doped Si substrate having a top 300 nm-thick layer of  $\text{SiO}_2$ . The graphene layers transferred onto the Si/ $\text{SiO}_2$  substrate were heated at 80  $^{\circ}\text{C}$  for 10 min to dry and then put in acetone for one day to completely dissolve the PMMA layer<sup>30,31</sup>. An artificial double-layer graphene was formed by subsequent transfer of another layer onto the first layer of graphene. After transferring and making the Hall bar of one graphene, then half part of it was removed with a combination of electron-beam lithography and oxygen plasma treatment, i.e. electron-beam lithography was used to expose the specified area of the graphene that was intended to be removed and oxygen plasma treatment was used to engrave that specified area. Each step of the process was carefully examined by microscope to verify the complete etching of graphene in the desired area. The second graphene layer was transferred thereafter and made a Hall bar with careful adjustments it was then aligned exactly on to the engraved graphene Hall bar. Therefore, we were able to examine the characteristics of double and single-layer graphene. The Cr/Au (5/30 nm) contacts were coated by using a thermal evaporation system.

**Device characterization and measurement setup.** Raman spectra were measured with a Renishaw microspectrometer over a wavenumber range from 1100 to 3200  $\text{cm}^{-1}$ , with a laser wavelength of 514.5 nm. The spot size was 1  $\mu\text{m}$  and the power was kept at 1.0 mW to avoid local heating. The electrical and magneto-transport properties of graphene junctions were measured using ac lock-in techniques at frequency of 11.7 Hz with the root-mean-square current amplitude of 50  $\mu\text{A}$ . Low temperature measurements were carried out in liquid helium cryostat (down to 4.2 K) with magnetic field up to 9 T. Lake Shore 331 temperature controller was utilized to modulate and control the temperature range.

## References

- Geim, A. K. & Novoselov, K. S. The rise of graphene. *Nat Mater* **6**, 183–191 (2007).
- Novoselov, K. S. *et al.* Unconventional quantum Hall effect and Berry's phase of  $2\pi$  in bilayers graphene. *Nat Phys* **2**, 177–180 (2006).
- McCann, E. & Fal'ko, V. I. Landau-level degeneracy and quantum hall effect in a graphite bilayers. *Phys Rev Lett* **96**, 086805 (2006).
- Ho, J. H., Lu, C. L., Hwang, C. C., Chang, C. P. & Lin, M. F. Coulomb excitations in AA- and AB-stacked bilayers graphites. *Phys Rev B* **74**, 085406 (2006).
- Nanda, B. R. K. & Satpathy, S. Strain and electric field modulation of the electronic structure of bilayers graphene. *Phys Rev B* **80**, 165430 (2009).
- Iqbal, M. Z. *et al.* Spin valve effect of NiFe/graphene/NiFe junctions. *Nano Research* **6**, 373–380 (2013).
- Iqbal, M. Z., Iqbal, M. W., Jin, X., Hwang, C. & Eom, J. Interlayer dependent polarity of magnetoresistance in graphene spin valves. *Journal of Materials Chemistry C* **3**, 298–302 (2015).
- Mucha-Kruczynski, M., Aleiner, I. L. & Fal'ko, V. I. Strained bilayers graphene: Band structure topology and Landau level spectrum. *Phys Rev B* **84**, 041404R (2011).
- Son, Y. W., Choi, S. M., Hong, Y. P., Woo, S. & Jhi, S. H. Electronic topological transition in sliding bilayers graphene. *Phys Rev B* **84**, 155410 (2011).

10. dos Santos, J. M. B. L., Peres, N. M. R. & Castro, A. H. Graphene bilayers with a twist: Electronic structure. *Phys Rev Lett* **99**, 256802 (2007).
11. Bistrizter, R. & MacDonald, A. H. Moire bands in twisted double-layer graphene. *P Natl Acad Sci USA* **108**, 12233–12237 (2011).
12. Mele, E. J. Band symmetries and singularities in twisted multilayer graphene. *Phys Rev B* **84**, 235439 (2011).
13. Fallahazad, B. *et al.* Quantum Hall effect in Bernal stacked and twisted bilayers graphene grown on Cu by chemical vapor deposition. *Phys Rev B* **85**, 201408 (2012).
14. Chae, D.-H., Zhang, D., Huang, X. & von Klitzing, K. Electronic transport in two stacked graphene monolayers. *Nano Lett* **12**, 3905–3908 (2012).
15. Lee, D. S. *et al.* Quantum hall effect in twisted bilayers graphene. *Phys Rev Lett* **107**, 216602 (2011).
16. Kim, K. S. *et al.* Coexisting massive and massless Dirac fermions in symmetry-broken bilayers graphene. *Nat Mater* **12**, 887–892 (2013).
17. Boebinger, G. S., Jiang, H. W., Pfeiffer, L. N. & West, K. W. Magnetic-Field-Driven Destruction of Quantum Hall States in a Double Quantum-Well. *Phys Rev Lett* **64**, 1793–1796 (1990).
18. Gramila, T. J., Eisenstein, J. P., Macdonald, A. H., Pfeiffer, L. N. & West, K. W. Mutual Friction between Parallel 2-Dimensional Electron-Systems. *Phys Rev Lett* **66**, 1216–1219 (1991).
19. Eisenstein, J. P. & MacDonald, A. H. Bose-Einstein condensation of excitons in bilayers electron systems. *Nature* **432**, 691–694 (2004).
20. Castro Neto, A. H., Guinea, F., Peres, N. M. R., Novoselov, K. S. & Geim, A. K. The electronic properties of graphene. *Rev Mod Phys* **81**, 109–162 (2009).
21. Dresselhaus, M. S. & Dresselhaus, G. Intercalation compounds of graphite. *Adv Phys* **51**, 1–186 (2002).
22. Lu, C.-C. *et al.* Twisting bilayers graphene superlattices. *ACS nano* **7**, 2587–2594 (2013).
23. Novoselov, K. S. *et al.* Two-dimensional gas of massless Dirac fermions in graphene. *Nature* **438**, 197–200 (2005).
24. Iqbal, M. Z. *et al.* Enhanced intervalley scattering in artificially stacked double-layer graphene. *New J Phys* **16**, 083020 (2014).
25. Schmidt, H., Lüdtke, T., Barthold, P. & Haug, R. Mobilities and scattering times in decoupled graphene monolayers. *Physical review B* **81**, 121403 (2010).
26. Sanchez-Yamagishi, J. D. *et al.* Quantum Hall effect, screening, and layer-polarized insulating states in twisted bilayers graphene. *Physical review letters* **108**, 076601 (2012).
27. Schmidt, H., Lüdtke, T., Barthold, P. & Haug, R. Temperature dependent measurements on two decoupled graphene monolayers. *Physica E: Low-dimensional Systems and Nanostructures* **42**, 699–702 (2010).
28. Choi, M.-Y., Hyun, Y.-H. & Kim, Y. Angle dependence of the Landau level spectrum in twisted bilayers graphene. *Physical review B* **84**, 195437 (2011).
29. Wang, Z., Liu, F. & Chou, M. Fractal Landau-level spectra in twisted bilayers graphene. *Nano letters* **12**, 3833–3838 (2012).
30. Kim, K. S. *et al.* Large-scale pattern growth of graphene films for stretchable transparent electrodes. *Nature* **457**, 706–710 (2009).
31. Xue, Y. Z. *et al.* Synthesis of large-area, few-layer graphene on iron foil by chemical vapor deposition. *Nano Res* **4**, 1208–1214 (2011).

## Acknowledgements

This research was supported by Nano-Material Technology Development Program (2012M3A7B4049888) through the National Research Foundation of Korea (NRF) funded by the Ministry of Science, ICT and Future Planning. This research was also supported by Priority Research Center Program (2010-0020207) and the Basic Science Research Program (2013R1A1A2061396) through NRF funded by the Ministry of Education. The authors would also like to extend their sincere appreciation to the Deanship of Scientific Research at King Saud University for funding this research group no. RG1435-004.

## Author Contributions

M.Z.I. and J.E. conceived and designed the study. M.Z.I. worked on device characteristics, data collection, analysis, and interpretation of results. M.Z.I. performed device fabrication, and M.W.I., S.S. and M.F.K. helped during device fabrication process. J.N. and K.S.K. grow the graphene. S.S. and S.M.R. helped during data interpretation. M.Z.I. wrote the manuscript. All authors contributed to discussion and reviewed the manuscript.

## Additional Information

**Competing financial interests:** The authors declare no competing financial interests.

**How to cite this article:** Iqbal, M. Z. *et al.* Interaction driven quantum Hall effect in artificially stacked graphene bilayers. *Sci. Rep.* **6**, 24815; doi: 10.1038/srep24815 (2016).



This work is licensed under a Creative Commons Attribution 4.0 International License. The images or other third party material in this article are included in the article's Creative Commons license, unless indicated otherwise in the credit line; if the material is not included under the Creative Commons license, users will need to obtain permission from the license holder to reproduce the material. To view a copy of this license, visit <http://creativecommons.org/licenses/by/4.0/>